Pattern Discrimination of Neuroelectric Waveforms Evoked By Synchronized Visuo-Motor Integration†

Sina Khanmohammadi[1], Vladimir Miskovic[2], Farnaz Zamani Esfahlani[3], and Chun-An Chou[1*]

***Abstract*— Today, there is a significant demand for fast, accurate, and automated methods for the discrimination of latent patterns in neuroelectric waveforms. One of the main challenges is the development of efficient feature extraction tools to utilize the rich spatio-temporal information inherent in large scale human electrocortical activity. In this paper, our aim is to isolate the most suitable feature extraction method for accurate classification of EEG data related to distinct modes of sensorimotor integration. Our results demonstrate that with some user-dependent input for feature space constraint, a simple classification framework can be developed to accurately distinguish between brain electrical activity patterns during two distinct conditions.**

I. INTRODUCTION

Recording electroencephalography (EEG) provides a direct index of neuronal activity averaged across large populations of synchronously active pyramidal cells in the human cortex [1]. Scalp-recorded patterns of neuroelectrical potentials exhibit dynamic fluctuations in regional and network functional activity when individuals engage in distinct cognitive and perceptual tasks. Given the multi-dimensional nature of EEG recordings and the remarkable variety of quantitative features that can be extracted even from spontaneous (resting) EEG recordings, an important question is related to the relative information yield of these various measures. Specifically, to what extent can we use the rich spatio-temporal patterns of EEG waveforms to discriminate distinct modes of large-scale cortical activity between different experimental conditions. In the present experiment, we sought to employ a data-driven approach for the latent classification of two distinct information processing modes (one related to simple viewing of an object, the other to the performance of a demanding visuo-motor tracking task). To this end, we recorded dense-array event-related EEG activity while the observers engaged in a visuo-motor integration task versus a passive viewing control condition. We recorded steady-state visual evoked potentials (ssVEPs) which are large-scale oscillatory field potentials elicited by a rhythmic train of sensory stimulation. The human visual cortex exhibits so-called resonance phenomena [2], which consists of entrained spectral response signatures to stimuli that have a constant rate of luminance or contrast modulation. In this paper, we exploit the high signal-to-noise ratio and narrow-band manifestations of ssVEPs to focus on the extraction of relevant event-related EEG dynamics.

†This work is supported by the Grant (I920247) at Binghamton University.

[1]S. Khanmohammadi and C.-A. Chou* are with Department of Systems Science and Industrial Engineering, SUNY Binghamton, Binghamton, NY-13902, USA (Asterisk indicates the corresponding author. Tel:607-777-5930, Email: cachou@binghamton.edu)

[2]V. Miskovic is with Department of Psychology, SUNY Binghamton, Binghamton, NY-13902, USA

[3]F. Zamani Esfahlani is with Department of Bioengineering, SUNY Binghamton, Binghamton, NY-13902, USA

II. METHODOLOGY

The overall framework (shown in Fig. 1) consists of steps including data acquisition, data preprocessing, feature extraction, and classification. Each of these steps are described greater detail below.

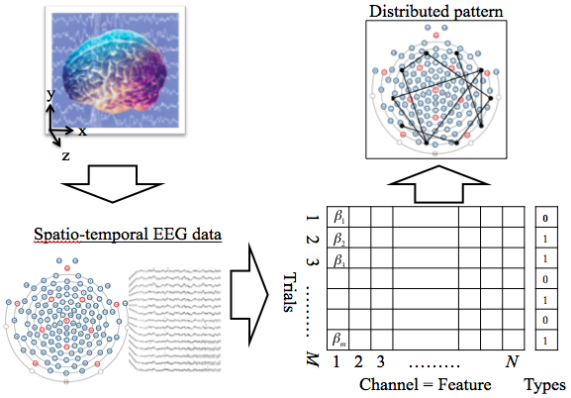

Fig. 1: Overview of implementation framework.

A. Data Acquisition

The experiment included two male observers who provided consent prior to taking part in the study. The observers had corrected to normal vision and no family history of photic epilepsy. Given the small number of observers, the primary objective of this paper was to establish a benchmark validation with real electrophysiological data before proceeding to a larger dataset. Observers were seated in a comfortable chair in a dimly lit room and a dense-array electroencephalogram (EEG) sensor net was applied. Observers were given instructions to fixate on the center of the display and avoid eye movements and blinks. Stimuli were displayed on a $23inch$ LED monitor (Samsung S23A750D) with a $120Hz$ refresh rate, positioned at a distance of $1m$. The experimental task consisted of two separate conditions. In the control condition, observers viewed one shape (circle or square, counterbalanced across the two observers) that was shown for 5 duty cycles of the LED display and removed for 5 subsequent duty cycles, leading to an on-off (square-wave) flicker rate of $12Hz$. Importantly, the color of the shape also

changed (from gray to green) every $1000ms$. In the visuo-motor condition, observers viewed a distinct shape (circle or square, depending on experimental assignment) but were instructed to produce 3 finger taps using the right hand during each color cycle (i.e., a $3Hz$ finger tap rate during the green phase, a new $3Hz$ finger tap rate during the white phase and so on). The visuo-motor condition thus required active integration of the visual (rapidly occurring color changes) and motor (finger tap) task components. Stimuli were presented for 9 continuous seconds of viewing time, interspersed with blank inter-trial intervals varying randomly between 7 and 9 seconds. There were 20 experimental trials in each of the two conditions. The EEG was continuously recorded from 129 sensors using an Electrical Geodesics HydroCel Geodesic Sensor Net digitized online at a rate of $250Hz$, using the vertex sensor (Cz) as the recording reference, with the online band-pass filter set at $50Hz$ (low-pass). Sensor impedances were kept below $50k\Omega$.

B. Data Preprocessing

Offline EEG analyses were implemented using the ElectroMagnetoEncephalography (EMEGS) toolbox for MATLAB [3]. Relative to stimulus onset, epochs were extracted from the raw EEG signals that included $500ms$ pre- and $9000ms$ post-onset for all conditions. As described by [4], statistical parameters were used to calculate distributions across trials and channels, and interpolate artifact-contaminated channels. The original recording reference (Cz) was first used to detect recording artifacts, and then the data was average referenced to detect global artifacts. Rejection criteria included the maximum of the amplitude, standard deviation, and first temporal derivate in a given trial-channel pair. Subsequently, the artifact-clean scalp EEG data were submitted to a Laplacian transform to calculate current source density (CSD) estimates. An important advantage of the CSD transform is that it provides a reference-independent estimate of electrocortical activity. Here, we implemented the CSD approach described by [5], which is based on spherical spline interpolation and well suited for dense-array EEG montages. To eliminate non-stationary (onset event-related potential) data, we eliminated the first $1000ms$ post-stimulus onset. Therefore, the analyses presented here focus on steady-state EEG activity during the period from $1000ms$ to $9000ms$. At the end of the data preprocessing, for an observer, we obtain a three dimensional matrix $A = (a_{ijk})$, where $i = 1,...,M$, $j = 1,...,N$, and $k = 1,...,P$. Here M is the total number of time points (i.e. 2001), N is the total number of channels (i.e. 129), and P is the total number of trials. Each cell of matrix A represents the EEG signal values (amplitude).

C. Feature Extraction

Two feature extraction methods were applied to extract the representative values of channels: 1) Fast Fourier Transform (FFT) at $12Hz$ and 2) Discrete Wavelet Transform (DWT) at $7.81-15.62Hz$. Each of these feature extraction methods are described as follows:

1) Absolute value of Fast Fourier Transform at $12Hz$ (AFFT-12). In this feature extraction method, the Discrete Fourier Transform (DFT) of EEG signals in each channel j of each trial k is calculated using the Cooley-Tukey FFT algorithm [6]. Then, the absolute value of the DFT corresponding to the frequency of $12Hz$ was calculated to represent signals in that specific frequency bin. The DFT is expressed as:

$$X(q) = \sum_{i=1}^{M} x(i)\omega_M^{(i-1)(q-1)}, \qquad (1)$$

where $\omega_M = e^{\frac{(-2\pi i)}{M}}$ and $x(i)$ is a complex number.

2) Standard deviation of the detail coefficients of Discrete Wavelet Transform in α frequency band (α-DWT). In this feature extraction method EEG signals in each channel j of each trial k was decomposed into eight details ($D1-D8$), and one approximation ($A8$), using Daubechies 4 wavelet filter. Then, the standard deviation of the detail coefficients in $D4$ (where $D4$ corresponds to the α frequency band ($7.81-15.62Hz$) was calculated to represent signals in that specific frequency range. The DWT is expressed as [**?**]:

$$DWT(a,b) = \frac{1}{\sqrt{|2^a|}} \int_{-\infty}^{\infty} x(t)\psi(\frac{t-2^a b}{2^a})dt, \qquad (2)$$

where a and b are scaling and shifting parameters.

The output of feature extraction is presented as a $P \times (N+1)$ matrix A_f, where P represents the total number of trials in both experiments, and N represents the total number of channels. The $N+1$ column represents the type of experiments, where class 0 corresponds to the experiment for visual cortex activity and class 1 corresponds to the experiment for visual-motor cortex activity. Each cell in the A_f matrix denotes a feature value extracted from one of the above-mentioned methods, and it represents a column of matrix A (one channel). In short, the feature extraction is a mapping step from matrix A to matrix A_f.

To avoid bias caused by scale difference, the values in every column (for a channel) of the A_f matrix were normalized between 0 and 1.

D. Classification

After extracting the necessary features, supervised classification algorithms were applied to classify the trials into two experimental conditions, where one indicated the control (view only) and the other indicated the visuo-motor condition. The classification algorithms used in this study are linear classification algorithms that are arguably simpler, faster, and easier to interpret than non linear supervised classification methods. The three linear supervised classification algorithms used in this study are briefly described in this section. Readers are referred to [7], [8] for more details of supervised machine learning techniques.

1) Support Vector Machine (SVM) is arguably the most widely used algorithm to analyze brain activity data

because of its robustness and good generalization properties [9]. It performs well on the data with high feature-to-instance ratio (i.e. 129 to 27 in our data set). SVM is based on the concept of margin [7], where margin is defined as two sides of a hyperplane that can separate the data. The main goal of SVM is to identify a hyperplane with the largest margin, where the data can be linearly separated using this identified hyperplane. In short, SVM is a linear discriminative classifier that uses a hyperplane to separate data into two groups in a way that the margin between two classes are maximized [10].

2) Logistic Regression (LR) is another linear discriminative classifier, whose underlying intuition is to separate the data instances into two groups using a hyperplane [10]. LR is based on a concept called logit [7], where logit is a linear transformation for the probability value. The term logistic in logistic regression indicates the fact that logit function is solved using a linear function. Apart from working substantially well in the datasets with high feature-to-instance ratio, one of the main advantages of the logistic regression is the fact that it provides a probability value associated with the predicted class of a new data point.
3) Linear Discriminant Analysis (LDA) is a classification method based on transferring the feature space into a new lower dimension subspace [7]. The goal is to maximize the ratio of class variance to within class variance in the dataset, which guarantees maximal separability. Discriminant analysis assumes that the data corresponding to different classes follow different Gaussian distributions. LDA is one of the most popular classification algorithms in EEG data analysis, mainly because of its simplicity and computational speed that makes it suitable for brain computer interface (BCI) applications [11].

To evaluate the classification performance, a leave-one-out cross validation framework is employed where in an iteration, one trial is used as testing data while the remaining trials are used as training data. The accuracy is calculated by taking the correctly classified trials divided by the total number of trials.

III. RESULTS

The three linear classification algorithms (SVM, LR, and LDA) were applied to the outputs of the two different feature extraction methods, using different channel selection strategies. The channel selections included: selection of all 129 channels, selection of channels based on expert knowledge (user-guided selection of channels corresponding to regions that were proximal to the visual and motor cortices), three groups of randomly selected channels each containing fifteen channels that were not included in the user-guided selection, and top fifteen channels based on the Pearson correlation between each channel and class label. The selected channels for the experiment are presented in Table I. The details of the experimental results are provided in Tables 2-4 for observer 01, observer 02, and a combination of both observers. Each table provides the result in terms of classification accuracy (%) and ranking (smaller rank index means higher accuracy). Additionally, average rank is provided based on the individual rankings in each table. The average rank indicates how well one specific classification algorithm performed for one channel selection group, using two feature extraction methods. The best ranking for each classification algorithm is highlighted using underline.

TABLE I: Indexes of Selected Channels Included in Classification Models.

Selected channels	Index of channels included in classification
All channels	[1 *to* 129]
Expert Selection (Visual/Left Motor)	[70, 71, 74, 76, 83, 82, 81, 75, 36, 37, 42, 30, 29, 35, 41]
Expert Selection (Visual)	[70, 71, 74, 76, 83, 82, 81, 75]
Expert Selection (Left Motor)	[36, 37, 42, 30, 29, 35, 41]
Expert Selection (Right Motor)	[87, 93, 103, 104, 105, 110, 111]
Expert Selection (Frontal)	[18, 16, 10, 4, 5, 12, 19, 11]
Expert Selection (Left Motor/Right Motor)	[36, 37, 42, 30, 29, 35, 41, 93, 87, 105, 111, 110, 103, 104]
Random selection1	[21, 8, 9, 26, 33, 119, 59, 80, 54, 97, 46, 56, 84, 15, 121]
Random selection2	[32, 44, 27, 22, 114, 108, 79, 94, 58, 64, 125, 107, 61, 78, 109]
Random selection3	[128, 1, 3, 23, 39, 40, 7, 31, 55, 90, 101, 96, 63, 50, 120]

TABLE II: Classification Results for Observer 01.

SVM	**AFFT-12 Acc (Rank)**	**α-DWT Acc (Rank)**	**Avg Rank**
All Channels	48.15% (9)	88.89% (2)	5.5
Expert Selection (Visual/Left Motor)	66.67% (5)	74.07% (6)	5.5
Expert Selection (Visual)	59.26% (6)	48.15% (9)	7.5
Expert Selection (Left Motor)	81.48% (1)	74.07% (6)	3.5
Expert Selection (Right Motor)	70.37% (2)	85.19% (4)	3.0
Expert Selection (Frontal)	51.85% (8)	62.96% (8)	8.0
Expert Selection (Left Motor/Right Motor)	70.37% (2)	100.00% (1)	**1.5**
Average Random Selection	59.26% (6)	85.19% (4)	5.0
Top Ranked Channels (Based on Correlation)	70.37% (2)	88.89% (2)	2.0
LR	**AFFT-12 Acc (Rank)**	**α-DWT Acc (Rank)**	**Avg Rank**
All Channels	55.56% (8)	70.37% (6)	7.0
Expert Selection (Visual/Left Motor)	66.67% (3)	59.26% (8)	5.5
Expert Selection (Visual)	70.37% (1)	44.44% (9)	5.0
Expert Selection (Left Motor)	70.37% (1)	70.37% (6)	3.5
Expert Selection (Right Motor)	62.96% (4)	92.59% (1)	**2.5**
Expert Selection (Frontal)	40.74% (9)	81.48% (4)	6.5
Expert Selection (Left Motor/Right Motor)	62.96% (4)	92.59% (1)	**2.5**
Average Random Selection	56.79% (7)	75.31% (5)	6.0
Top Ranked Channels (Based on Correlation)	59.26% (6)	85.19% (3)	4.5
LDA	**AFFT-12 Acc (Rank)**	**α-DWT Acc (Rank)**	**Avg Rank**
All Channels	40.74% (8)	85.19% (3)	5.5
Expert Selection (Visual/Left Motor)	66.67% (3)	59.26% (8)	5.5
Expert Selection (Visual)	70.37% (1)	44.44% (9)	5.0
Expert Selection (Left Motor)	70.37% (1)	70.37% (7)	4.0
Expert Selection (Right Motor)	62.96% (4)	92.59% (1)	**2.5**
Expert Selection (Frontal)	40.74% (8)	81.48% (5)	6.5
Expert Selection (Left Motor/Right Motor)	62.96% (4)	92.59% (1)	**2.5**
Average Random Selection	56.79% (7)	75.31% (6)	6.5
Top Ranked Channels (Based on Correlation)	59.26% (6)	85.19% (3)	4.5

From Tables 2-4, it shows that the expert selected channel clusters (where the cluster corresponds to expected active regions of the brain) provided a very good accuracy compared to other groups of selected channels. More specifically, in six out of nine tests, the expert selection of channels resulted in best ranking when compared to other channel selection methods.

Top channels for each feature extraction method based on the (Pearson) correlation between channels and class, and the regions corresponding to expert selection of channels is shown in Fig 2. It can be observed that the most informative channels in terms of classification performance are located close to motor cortex, which was expected considering the nature of the synchronized visuo-motor integration task.

IV. CONCLUSION

The current study used a simple classification framework to distinguish between two types of EEG patterns

TABLE III: Classification Results for Observer 02.

SVM	AFFT-12 Acc (Rank)	α-DWT Acc (Rank)	Avg Rank
All Channels	61.54% (2)	80.77% (4)	3.0
Expert Selection (Visual/Left Motor)	53.85% (7)	80.77% (4)	5.5
Expert Selection (Visual)	42.31% (8)	53.85% (8)	8.0
Expert Selection (Left Motor)	61.54% (2)	84.62% (1)	1.5
Expert Selection (Right Motor)	30.77% (9)	76.92% (6)	7.5
Expert Selection (Frontal)	61.54% (2)	53.85% (8)	5.0
Expert Selection (Left Motor/Right Motor)	57.69% (6)	84.62% (1)	3.5
Average Random	58.97% (5)	74.36% (7)	6.0
Top Ranked Channels (Based on Correlation)	76.92% (1)	84.62% (1)	**1.0**
LR	**AFFT-12 Acc (Rank)**	**α-DWT Acc (Rank)**	**Avg Rank**
All Channels	50.00% (8)	65.38% (6)	7.0
Expert Selection (Visual/Left Motor)	53.85% (7)	65.38% (6)	6.5
Expert Selection (Visual)	50.00% (8)	61.54% (9)	8.5
Expert Selection (Left Motor)	57.69% (4)	73.08% (3)	3.5
Expert Selection (Right Motor)	69.23% (2)	76.92% (2)	**2.0**
Expert Selection (Frontal)	57.69% (4)	65.38% (6)	5.0
Expert Selection (Left Motor/Right Motor)	65.38% (3)	80.77% (1)	**2.0**
Average Random	55.13% (6)	69.23% (5)	5.5
Top Ranked Channels (Based on Correlation)	73.08% (1)	73.08% (3)	**2.0**
LDA	**AFFT-12 Acc (Rank)**	**α-DWT Acc (Rank)**	**Avg Rank**
All Channels	46.15% (9)	100.00% (1)	5.0
Expert Selection (Visual/Left Motor)	53.85% (7)	65.38% (7)	7.0
Expert Selection (Visual)	50.00% (8)	61.54% (9)	8.5
Expert Selection (Left Motor)	57.69% (4)	73.08% (4)	4.0
Expert Selection (Right Motor)	69.23% (2)	76.92% (3)	**2.5**
Expert Selection (Frontal)	57.69% (4)	65.38% (7)	5.5
Expert Selection (Left Motor/Right Motor)	65.38% (3)	80.77% (2)	**2.5**
Average Random	55.13% (6)	69.23% (6)	6.0
Top Ranked Channels (Based on Correlation)	73.08% (1)	73.08% (4)	**2.5**

TABLE IV: Classification Results for the combination of Observers 01 and 02.

SVM	AFFT-12 Acc (Rank)	αDCDW Acc (Rank)	Avg Rank
All Channels	62.26% (2)	73.58% (1)	**1.5**
Expert Selection (Visual/Left Motor)	64.15% (1)	67.92% (3)	2.0
Expert Selection (Visual)	52.83% (8)	64.15% (5)	6.5
Expert Selection (Left Motor)	56.60% (7)	67.92% (3)	5.0
Expert Selection (Right Motor)	60.38% (4)	64.15% (5)	4.5
Expert Selection (Frontal)	62.26% (2)	64.15% (5)	3.5
Expert Selection (Left Motor/Right Motor)	50.94% (9)	60.38% (9)	9.0
Average Random Selection	58.49% (5)	68.55% (2)	3.5
Top Ranked Channels (Based on Correlation)	58.49% (5)	64.15% (5)	5.0
LR	**AFFT12 Acc (Rank)**	**αDCDW Acc (Rank)**	**Avg Rank**
All Channels	54.72% (6)	66.04% (2)	4.0
Expert Selection (Visual/Left Motor)	52.83% (8)	62.26% (6)	7.0
Expert Selection (Visual)	54.72% (6)	58.49% (8)	7.0
Expert Selection (Left Motor)	58.49% (3)	66.04% (2)	2.5
Expert Selection (Right Motor)	62.26% (1)	60.38% (7)	4.0
Expert Selection (Frontal)	58.49% (3)	54.72% (9)	6.0
Expert Selection (Left Motor/Right Motor)	56.60% (5)	66.04% (2)	3.5
Average Random Selection	59.12% (2)	66.67% (1)	**1.5**
Top Ranked Channels (Based on Correlation)	49.06% (9)	64.15% (5)	7.0
LDA	**AFFT-12 Acc (Rank)**	**αDCDW Acc (Rank)**	**Avg Rank**
All Channels	52.83% (7)	66.04% (2)	4.5
Expert Selection (Visual/Left Motor)	52.83% (7)	62.26% (6)	6.5
Expert Selection (Visual)	56.60% (5)	58.49% (8)	6.5
Expert Selection (Left Motor)	58.49% (3)	66.04% (2)	2.5
Expert Selection (Right Motor)	62.26% (1)	60.38% (7)	4.0
Expert Selection (Frontal)	58.49% (3)	54.72% (9)	6.0
Expert Selection (Left Motor/Right Motor)	56.60% (5)	66.04% (2)	3.5
Average Random Selection	59.12% (2)	66.67% (1)	**1.5**
Top Ranked Channels (Based on Correlation)	49.06% (9)	64.15% (5)	7.0

corresponding to a simple viewing versus a complex visuo-motor integration condition. The results are encouraging and suggest that with the help of user-dependent channel selection, we can accurately discriminate between these two neuroelectric waveform patterns. The results were not consistent for combination of subject one and two (Table 4), which suggest additional steps should be taken to generalize EEG classification results across multiple subjects. Our next step will be to address this issue and expand this framework to study functional connectivity among cortical regions. Of interest, the channels with the greatest discrimination accuracy between the two conditions were those located over anterior scalp regions overlying the motor and premotor cortex.

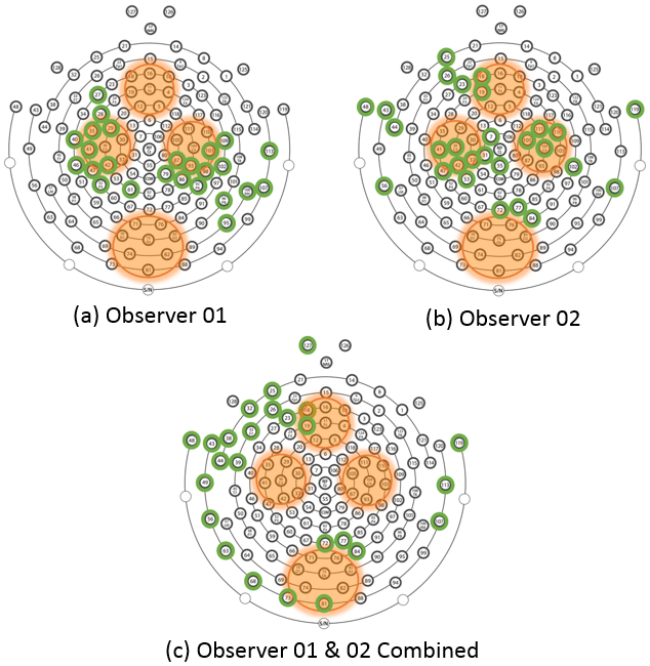

Fig. 2: Illustrations of top ranked channels (in green) based on the Pearson correlation to the class, compared to expert selected channels (in orange regions), for observer 01, 02, and the combination of observers 01 and 02. The 129 channel map was retrieved from [12].

REFERENCES

[1] P. L. Nunez, "Toward a quantitative description of large-scale neocortical dynamic function and eeg," *Behavioral and Brain Sciences*, vol. 23, no. 03, pp. 371–398, 2000.

[2] C. S. Herrmann, "Human eeg responses to 1–100 hz flicker: resonance phenomena in visual cortex and their potential correlation to cognitive phenomena," *Experimental brain research*, vol. 137, no. 3-4, pp. 346–353, 2001.

[3] P. Peyk, A. De Cesarei, and M. Junghöfer, "Electromagnetoencephalography software: overview and integration with other eeg/meg toolboxes," *Computational intelligence and neuroscience*, vol. 2011, 2011.

[4] M. Junghöfer, T. Elbert, D. M. Tucker, and B. Rockstroh, "Statistical control of artifacts in dense array eeg/meg studies," *Psychophysiology*, vol. 37, no. 4, pp. 523–532, 2000.

[5] M. Junghöfer, T. Elbert, P. Leiderer, P. Berg, and B. Rockstroh, "Mapping eeg-potentials on the surface of the brain: a strategy for uncovering cortical sources," *Brain Topography*, vol. 9, no. 3, pp. 203–217, 1997.

[6] J. W. Cooley and J. W. Tukey, "An algorithm for the machine calculation of complex fourier series," *Math. comput*, vol. 19, no. 90, pp. 297–301, 1965.

[7] S. B. Kotsiantis, "Supervised machine learning: a review of classification techniques." *Informatica (03505596)*, vol. 31, no. 3, 2007.

[8] C. C. Aggarwal and C. Zhai, "A survey of text classification algorithms," in *Mining text data*. Springer, 2012, pp. 163–222.

[9] F. Pereira, T. Mitchell, and M. Botvinick, "Machine learning classifiers and fmri: a tutorial overview," *Neuroimage*, vol. 45, no. 1, pp. S199–S209, 2009.

[10] C. Chou, K. Kampa, S. Mehta, R. Tungaraza, W. Chaovalitwongse, and T. Grabowski, "Voxel selection framework in multi-voxel pattern analysis of fmri data for prediction of neural response to visual stimuli," 2010.

[11] C. Vidaurre, A. Schlogl, R. Cabeza, R. Scherer, and G. Pfurtscheller, "Study of on-line adaptive discriminant analysis for eeg-based brain computer interfaces," *Biomedical Engineering, IEEE Transactions on*, vol. 54, no. 3, pp. 550–556, 2007.

[12] E. M. D. Company, "128-channel map," http://www.egi.com/, accessed: 2014-03-13.